mathematics

Article

An Efficient Linearized Difference Algorithm for a Diffusive Sel′kov–Schnakenberg System

Yange Wang [1] **and Xixian Bai** [2,*]

[1] School of Computer Science, Zhengzhou University of Economics and Business, Zhengzhou 451191, China; wyg0610@163.com
[2] School of Mathematics and Statistics, Zhengzhou University, Zhengzhou 450001, China
* Correspondence: xixianmath@zzu.edu.cn

Abstract: This study provides an efficient linearized difference algorithm for a diffusive Sel′kov–Schnakenberg system. The algorithm is developed by using a finite difference method that relies on a three-level linearization approach. The boundedness, existence and uniqueness of the solution of our proposed algorithm are proved. The numerical experiments not only validate the accuracy of the algorithm but also preserve the Turing patterns.

Keywords: finite difference method; Sel′kov–Schnakenberg system; boundedness; existence and uniqueness

MSC: 65M06

check for updates

Citation: Wang, Y.; Bai, X. An Efficient Linearized Difference Algorithm for a Diffusive Sel′kov–Schnakenberg System. *Mathematics* **2024**, *12*, 894. https://doi.org/10.3390/math12060894

Academic Editors: Qinghe Yao and Patricia J. Y. Wong

Received: 2 February 2024
Revised: 5 March 2024
Accepted: 15 March 2024
Published: 18 March 2024

Copyright: © 2024 by the authors. Licensee MDPI, Basel, Switzerland. This article is an open access article distributed under the terms and conditions of the Creative Commons Attribution (CC BY) license (https://creativecommons.org/licenses/by/4.0/).

1. Introduction

The occurrence of oscillatory patterns, multiple steady-state solutions and chaotic behaviors is a fascinating phenomenon observed across numerous chemical, biological and physical systems [1,2]. Turing's theory reveals the principles of the relationship between the patterns produced by convection–diffusion systems and these phenomena [3]. As a famous example related to cellular processes in biochemical systems, the Sel′kov–Schnakenberg system has attracted the attention of many scholars on the stability and the existence of steady-state solutions [4–7].

The Sel′kov–Schnakenberg model, as an extension of the Sel'kov model [8] and Schnakenberg model [9], can describes the limit cycle behavior:

$$A \rightleftharpoons V, B \rightleftharpoons U, 2U + V \rightleftharpoons 3U, \tag{1}$$

where A and B are the chemical sources of V and U, respectively. U is the auto-catalyst, and V is the reactant. The mathematical modeling of the process leads to the following Sel′kov–Schnakenberg system [10]:

$$\begin{cases} u_t = d_1\Delta u - u + u^2 v + b + av, \ x \in \Omega, \ t > 0, & (2) \\ v_t = d_2 \Delta v + \lambda - u^2 v - av, \qquad x \in \Omega, \ t > 0, & (3) \end{cases}$$

where u represents the concentration of the auto-catalyst, and v represents the concentration of the reactant. Their corresponding diffusion coefficients are denoted by d_1 and d_2, respectively. The variables x and t are time and space variables, respectively. The dimensionless constant rate for the low activity state is given by a, and b and λ represent dimensionless chemical sources, with $a, b \geq 0$ and $\lambda > 0$.

With the homogeneous Neumann boundary conditions:

$$\frac{\partial u}{\partial \mathbf{n}} = \frac{\partial v}{\partial \mathbf{n}} = 0, \ on \ \partial\Omega \times (0, T), \tag{4}$$

and initial conditions

$$u(x,0) = \phi(x),\ v(x,0) = \psi(x),\ x \in \Omega, \tag{5}$$

where $\partial\Omega$ represents the boundary of domain Ω, and $\mathbf{n}$ denotes the outward unit normal vector of $\partial\Omega$.

Numerous works in the literature are devoted to the study of (2)–(5), including the Sel′kov model and the Schnakenberg model; See [1,2,7,10–14], and the references therein. In 2015, Zhou and Shi [14] investigate stability, instability, time-periodic orbits and spatiotemporal patterns through bifurcation methods and Leray–Schauder degree theory. In 2017, Li and Wang [12] focused on Sel′kov–Schnakenberg systems, explored steady-state issues, and provided the criteria for the formation of spatial patterns (especially Turing patterns) based on the results of the presence and absence of non-constant steady states. In 2014, Uecker and Wetzel [1] analyzed the patterns of the Sel′kov–Schnakenberg system in two dimensions by using the pde2path [15] finite element software package, numerically calculating embedded branches, such as hexagons in stripes. In 2021, Al Noufaey [2] used the Galerkin method to study the singularity behavior and stability of the Sel′kov–Schnakenberg system. In 2023, Wang and Zhou et al. [7] studied the Turing instability (diffusion drive) causing spatial patterns and obtained the conditions for the existence of Turing bifurcations, then the changes in the spatiotemporal pattern that depend on the parameters were theoretically analyzed, and a series of numerical experimental simulations were conducted to verify the analysis results through the finite difference method. To the best of our knowledge, there is relatively limited research on numerical algorithms for the Sel′kov–Schnakenberg system at present.

In view of the difficulties caused by nonlinear terms in the Sel′kov–Schnakenberg system, in this paper, we primarily focus on investigating a linearized finite difference algorithm. Taking into account the characteristics of Neumann boundary conditions, we explore the construction of a three-level linearized finite difference algorithm. Then, we provide a rigorous theoretical analysis of the boundedness, existence and uniqueness of the solutions for our proposed algorithm. Numerical results will demonstrate that the algorithm has second-order accuracy in both time and space, and we explore the spatial patterns of the system solutions.

The structure of this paper is as follows: In Section 2, we recall some fundamental notations and lemmas. In Section 3, a three-level finite difference algorithm is constructed in detail. The boundedness, existence and uniqueness of solutions are proved in detail for our algorithm in Section 4. Two numerical examples are provided to verify the efficiency of the algorithm and the theoretical analysis results in Section 5. Finally, we present conclusions in Section 6.

2. Preliminaries

In this section, we review some notations and lemmas that will be used in the remainder of the paper.

We will divide the domain $[L,R] \times [0,T]$. Take positive integers m, n, divide the domain $[L,R]$ into m equal parts, and divide the domain $[0,T]$ into n equal parts. The mesh size and nodes are denoted as follows:

$$\begin{aligned} h = (R-L)/m,\ \ x_i = ih, 0 \le i \le m. \\ \tau = T/n,\ \ t_k = k\tau, 0 \le k \le n. \end{aligned}$$

Denote

$$\begin{aligned} \delta_x u_{i+\frac{1}{2}} &= \frac{u_{i+1} - u_i}{h}, & \delta_x^2 u_i &= \frac{u_{i-1} - 2u_i + u_{i+1}}{h^2}, \\ u^{\bar{k}} &= \frac{u^{k+1} + u^k}{2}, & \Delta_t u^k &= \frac{u^{k+1} - u^{k-1}}{2\tau}. \end{aligned}$$

For convenience, we introduce the inner product $(\cdot,\cdot)$:

$$(u,v) = h(\frac{u_0v_0}{2} + \sum_{i=1}^{m-1} u_iv_i + \frac{u_mv_m}{2}),$$

then we define norms $\|\cdot\|, |\cdot|_1$:

$$\|u\| = \sqrt{(u,u)},$$
$$|u|_1 = \sqrt{h\sum_{i=1}^{m}(\delta_x u_{i-\frac{1}{2}})^2}.$$

Lemma 1 (See [16]). *Let a and b be the given constants, and $h > 0$.*
(1) If $g(x) \in C^3[c, c+h]$, then

$$g''(c) = \frac{2}{h}[\frac{g(c+h)-g(c)}{h} - g'(c)] - \frac{h}{3}g'''(\eta_1),\ c < \eta_1 < c+h, \tag{6}$$

If $g(x) \in C^4[c, c+h]$, then

$$g''(c) = \frac{2}{h}[\frac{g(c+h)-g(c)}{h} - g'(c)] - \frac{h}{3}g'''(c) - \frac{h^2}{12}g^{(4)}(\eta_2),\ c < \eta_2 < c+h. \tag{7}$$

(2) If $g(x) \in C^3[c-h, c]$, then

$$g''(c) = \frac{2}{h}[g'(c) - \frac{g(c)-g(c-h)}{h}] + \frac{h}{3}g'''(\eta_3),\ c-h < \eta_3 < c, \tag{8}$$

If $g(x) \in C^4[c-h, c]$, then

$$g''(c) = \frac{2}{h}[g'(c) - \frac{g(c)-g(c-h)}{h}] + \frac{h}{3}g'''(c) - \frac{h^2}{12}g^{(4)}(\eta_4), c-h < \eta_4 < c. \tag{9}$$

Lemma 2 (See [7]). *On the premise that the positive equilibrium*

$$E^*(u_*, v_*) = (\lambda + b, \frac{\lambda}{a + (b+\lambda)^2}),$$

of the corresponding local system is stable, for the Sel′kov–Schnakenberg system (2)–(5), the following hold:

1. *If $\lambda^2 - b^2 \leq a$, the positive Equilibrium E^* is asymptotically stable for all $d_1, d_2 > 0$.*
2. *If $\lambda^2 - b^2 > a$, we have the following results:*
   - (a) *When $\frac{d_2}{d_1} \leq \max\{1, \frac{(a+(\lambda+b)^2)^2}{\lambda^2-b^2-a}\}$, the positive equilibrium E^* is asymptotically stable.*
   - (b) *When $\frac{d_2}{d_1} > \max\{1, \frac{(a+(\lambda+b)^2)^2}{\lambda^2-b^2-a}\}$, and when $a > a_T$, the positive equilibrium E^* is asymptotically stable. And when $a < a_T$, the positive equilibrium E^* is unstable. When $a = a_T$ with $k = k_c$, the system undergoes Turing bifurcation, where a_T, k_c are the parameters in literature [7].*

3. A Three-Level Linearized Difference Algorithm

In this section, we will present the derivation process of our linearized difference algorithm.

Considering Equations (2) and (3) at the node (x_i, t_k), we have

$$\begin{cases} u_t(x_i,t_k) = d_1 u_{xx}(x_i,t_k) - u(x_i,t_k) + (u(x_i,t_k))^2 v(x_i,t_k) \\ \qquad +b + av(x_i,t_k),\ 0 \le i \le m,\ 1 \le k \le n-1, & (10) \\ v_t(x_i,t_k) = d_2 v_{xx}(x_i,t_k) + \lambda - (u(x_i,t_k))^2 v(x_i,t_k) \\ \qquad -av(x_i,t_k),\ 0 \le i \le m,\ 1 \le k \le n-1. & (11) \end{cases}$$

Applying numerical differentiation formulas to the above equations, it can be observed that

$$\Delta_t U_i^k = d_1 \delta_x^2 U_i^{\bar{k}} - U_i^{\bar{k}} + U_i^k V_i^k U_i^{\bar{k}} + b + aV_i^k + P_i^k, \qquad 1 \le i \le m-1,\ 1 \le k \le n-1, \quad (12)$$

$$\Delta_t V_i^k = d_2 \delta_x^2 V_i^{\bar{k}} + \lambda - (U_i^k)^2 V_i^{\bar{k}} - aV_i^{\bar{k}} + R_i^k, \qquad 1 \le i \le m-1,\ 1 \le k \le n-1. \quad (13)$$

Then, there exist constants c_1 and c_2 such that

$$|P_i^k| \le c_1(h^2 + \tau^2),\ 1 \le i \le m-1,\ 1 \le k \le n-1,$$
$$|R_i^k| \le c_2(h^2 + \tau^2),\ 1 \le i \le m-1,\ 1 \le k \le n-1.$$

Taking the derivative of both sides of the system of equations with respect to x, we have:

$$u_{xt} = d_1 u_{xxx} - u_x + 2uu_x v + u^2 v_x + av_x, \qquad x \in \Omega,\ t > 0,$$
$$v_{xt} = d_2 v_{xxx} - 2uu_x v - u^2 v_x - av_x, \qquad x \in \Omega,\ t > 0.$$

Applying boundary conditions (4), we obtain

$$u_{xxx}(L,t) = 0,\ u_{xxx}(R,t) = 0, 0 < t \le T, \quad (14)$$
$$v_{xxx}(L,t) = 0,\ v_{xxx}(R,t) = 0, 0 < t \le T. \quad (15)$$

Applying the boundary conditions (4), (14), (15) and using the Lemma 1, we can deduce

$$u_{xx}(L,t) = \frac{2}{h^2}[u(x_1,t) - u(x_0,t)] + \mathcal{O}(h^2),$$
$$u_{xx}(R,t) = -\frac{2}{h^2}[u(x_m,t) - u(x_{m-1},t)] + \mathcal{O}(h^2),$$
$$v_{xx}(L,t) = \frac{2}{h^2}[v(x_1,t) - v(x_0,t)] + \mathcal{O}(h^2),$$
$$v_{xx}(R,t) = -\frac{2}{h^2}[v(x_m,t) - v(x_{m-1},t)] + \mathcal{O}(h^2).$$

Therefore,

$$\begin{aligned} u_{xx}(L,t_{k+\frac{1}{2}}) &= \frac{1}{2}[u_{xx}(L,t_k) + u_{xx}(L,t_{k+1})] + \mathcal{O}(\tau^2) \\ &= \frac{1}{2}[\frac{2}{h^2}(U_1^k - U_0^k) + \frac{2}{h^2}(U_1^{k+1} - U_0^{k+1})] + \mathcal{O}(\tau^2 + h^2) \\ &= \frac{2}{h}\delta_x U_{\frac{1}{2}}^{\bar{k}} + \mathcal{O}(\tau^2 + h^2), \end{aligned} \quad (16)$$

$$\begin{aligned} u_{xx}(R,t_{k+\frac{1}{2}}) &= \frac{1}{2}[u_{xx}(R,t_k) + u_{xx}(R,t_{k+1})] + \mathcal{O}(\tau^2) \\ &= \frac{1}{2}[-\frac{2}{h^2}(U_m^k - U_{m-1}^k) - \frac{2}{h^2}(U_m^{k+1} - U_{m-1}^{k+1})] + \mathcal{O}(\tau^2 + h^2) \\ &= -\frac{2}{h}\delta_x U_{m-\frac{1}{2}}^{\bar{k}} + \mathcal{O}(\tau^2 + h^2). \end{aligned} \quad (17)$$

Employing a similar methodology, the result is

$$v_{xx}(L, t_{k+\frac{1}{2}}) = \frac{2}{h}\delta_x V^{\bar{k}}_{\frac{1}{2}} + \mathcal{O}(\tau^2 + h^2), \tag{18}$$

$$v_{xx}(R, t_{k+\frac{1}{2}}) = -\frac{2}{h}\delta_x V^{\bar{k}}_{m-\frac{1}{2}} + \mathcal{O}(\tau^2 + h^2). \tag{19}$$

Substituting $i = 0$ into Equation (10) and combining it with Equation (16), we derive

$$\Delta_t U_0^k = d_1 \frac{2}{h}\delta_x U^{\hat{k}}_{\frac{1}{2}} - U_0^{\bar{k}} + U_0^k V_0^k U_0^{\bar{k}} + b + aV_0^k + P_0^k,\ 1 \le k \le n-1. \tag{20}$$

Similarly, letting $i = m$ in Equation (10) and combining it with Equation (17), we obtain

$$\Delta_t U_m^k = -d_1 \frac{2}{h}\delta_x U^{\hat{k}}_{m-\frac{1}{2}} - U_m^{\bar{k}} + U_m^k V_m^k U_m^{\bar{k}} + b + aV_m^k + P_m^k,\ 1 \le k \le n-1, \tag{21}$$

where there exists a constant c_3 such that

$$|P_0^k| \le c_3(h^2 + \tau^2), 1 \le k \le n-1,$$
$$|P_m^k| \le c_3(h^2 + \tau^2), 1 \le k \le n-1.$$

Similar to the treatment of u, by substituting $i = 0$ into Equation (11) and combining it with Equation (18), we obtain

$$\Delta_t V_0^k = d_2 \frac{2}{h}\delta_x V^{\hat{k}}_{\frac{1}{2}} + \lambda - U_0^k V_0^k U_0^{\bar{k}} - aV_0^{\bar{k}} + R_0^k,\ 1 \le k \le n-1. \tag{22}$$

Letting $i = m$ in Equation (11) and combining it with Equation (19), we have

$$\Delta_t V_m^k = -d_2 \frac{2}{h}\delta_x V^{\hat{k}}_{m-\frac{1}{2}} + \lambda - (U_m^k)^2 V_m^{\bar{k}} - aV_m^{\bar{k}} + R_m^k,\ 1 \le k \le n-1, \tag{23}$$

where there exists a constant c_4 such that

$$|R_0^k| \le c_4(h^2 + \tau^2), 1 \le k \le n-1,$$
$$|R_m^k| \le c_4(h^2 + \tau^2), 1 \le k \le n-1.$$

From Equations (2) and (5), it follows that

$$u_t(x, 0) = d_1\phi_{xx}(x) - \phi(x) + \phi^2(x)\psi(x) + b + a\psi(x).$$

Then, we can obtain

$$U_i^1 = \phi(x_i) + \tau u_t(x_i, 0) + P_i^0,\ 0 \le i \le m, \tag{24}$$

where there exists a constant c_5 such that

$$|P_i^0| \le c_5\tau^2, \qquad 0 \le i \le m,$$
$$|\delta_x P^0_{i+\frac{1}{2}}| \le c_5\tau^2,\ 0 \le i \le m.$$

Deriving from Equations (3) and (5), we arrive

$$v_t(x, 0) = d_2\psi_{xx}(x) + \lambda - \phi^2(x)\psi(x) - a\psi(x).$$

Then, we can obtain

$$V_i^1 = \psi(x_i) + \tau v_t(x_i, 0) + R_i^0,\ 0 \le i \le m, \tag{25}$$

where there exists a constant c_6 such that

$$|R_i^0| \le c_6\tau^2, \qquad 0 \le i \le m,$$
$$|\delta_x R_{i+\frac{1}{2}}^0| \le c_6\tau^2,\ 0 \le i \le m.$$

Neglecting the infinitesimal terms in Equations (12), (13) and (20)–(25), we can establish the following three-level linearized difference algorithm for the Sel$'$kov–Schnakenberg system (2)–(5):

$$\begin{cases}
\Delta_t u_0^k = d_1 \frac{2}{h}\delta_x u_{\frac{1}{2}}^{\hat{k}} - u_0^{\bar{k}} + u_0^k v_0^k u_0^{\bar{k}} + b + a v_0^k, \quad 1 \le k \le n-1, & (26)\\
\Delta_t v_0^k = d_2 \frac{2}{h}\delta_x v_{\frac{1}{2}}^{\hat{k}} + \lambda - (u_0^k)^2 v_0^{\bar{k}} - a v_0^{\bar{k}}, 1 \le k \le n-1, & (27)\\
\Delta_t u_i^k = d_1 \delta_x^2 u_i^{\bar{k}} - u_i^{\bar{k}} + u_i^k v_i^k u_i^{\bar{k}} + b + a v_i^k, \quad 1 \le i \le m-1,\ 1 \le k \le n-1, & (28)\\
\Delta_t v_i^k = d_2 \delta_x^2 v_i^{\bar{k}} + \lambda - (u_i^k)^2 v_i^{\bar{k}} - a v_i^{\bar{k}}, \quad 1 \le i \le m-1,\ 1 \le k \le n-1, & (29)\\
\Delta_t u_m^k = -d_1 \frac{2}{h}\delta_x u_{m-\frac{1}{2}}^{\hat{k}} - u_m^{\bar{k}} + u_m^k v_m^k u_m^{\bar{k}} + b + a v_m^k, \quad 1 \le k \le n-1, & (30)\\
\Delta_t v_m^k = -d_2 \frac{2}{h}\delta_x v_{m-\frac{1}{2}}^{\hat{k}} + \lambda - (u_m^k)^2 v_m^{\bar{k}} - a v_m^{\bar{k}}, \quad 1 \le k \le n-1, & (31)\\
u_i^0 = \phi(x_i),\ v_i^0 = \psi(x_i), 0 \le i \le m, & (32)\\
u_i^1 = \phi(x_i) + \tau u_t(x_i, 0),\ 0 \le i \le m, & (33)\\
v_i^1 = \psi(x_i) + \tau v_t(x_i, 0),\ 0 \le i \le m. & (34)
\end{cases}$$

4. Theoretical Analysis

In this section, we will give a strict theoretical analysis of the boundedness, existence and uniqueness of the solutions to our proposed algorithm, respectively.

4.1. The Boundedness of Our Algorithm Solutions

Theorem 1. *Let $\{u_i^k, v_i^k\ |0 \le i \le m, 0 \le k \le n\}$ be solutions of the system (26)–(34). Then, there exist two constants c_7 and c_8 such that*

$$\|v^k\| \le c_7, \|u^k\| \le c_8, 0 \le k \le n. \tag{35}$$

Proof. From Equations (32)–(34), there exists a constant c_9 such that

$$\|u^0\| \le c_9, \|u^1\| \le c_9, \tag{36}$$
$$\|v^0\| \le c_9, \|v^1\| \le c_9. \tag{37}$$

Subsequently, Equations (26)–(31) can be collectively expressed as follows:

$$\Delta_t u_i^k = d_1 \delta_x^2 u_i^{\bar{k}} - u_i^{\bar{k}} + u_i^k v_i^k u_i^{\bar{k}} + b + a v_i^k, \qquad 0 \le i \le m,\ 1 \le k \le n-1, \tag{38}$$
$$\Delta_t v_i^k = d_2 \delta_x^2 v_i^{\bar{k}} + \lambda - (u_i^k)^2 v_i^{\bar{k}} - a v_i^{\bar{k}}, \qquad 0 \le i \le m,\ 1 \le k \le n-1. \tag{39}$$

Taking the inner product of $v_i^{\bar{k}}$ with Equation (39), we obtain

$$\begin{aligned}
&\frac{1}{4\tau}(\|v^{k+1}\|^2-\|v^{k-1}\|^2)\\
&=-d_2|v^{\bar{k}}|_1^2+(\lambda,v^{\bar{k}})-((u^k)^2v^{\bar{k}},v^{\bar{k}})-a\|v^{\bar{k}}\|^2\\
&\le(\lambda,v^{\bar{k}})\\
&\le\lambda\|v^{\bar{k}}\|\\
&\le\lambda\frac{\|v^{k+1}\|+\|v^{k-1}\|}{2},1\le k\le n-1.
\end{aligned}$$

Thus,

$$\|v^{k+1}\|-\|v^{k-1}\|\le 2\tau\lambda,\ 1\le k\le n-1.$$

Through recursion, it can be obtained

$$\begin{aligned}
\|v^k\|&\le 2\tau\lambda k+\|v^0\|\\
&\le 2T\lambda+\|v^0\|,\ 1\le k\le n.
\end{aligned}$$

Noting inequality (37), it can be derived that

$$\|v^k\|\le c_7,0\le k\le n. \tag{40}$$

Taking the inner product of $u_i^{\bar{k}}$ with Equation (38), we obtain

$$\begin{aligned}
&\frac{1}{4\tau}(\|u^{k+1}\|^2-\|u^{k-1}\|^2)\\
&=-d_1|u^{\bar{k}}|_1^2-\|u^{\bar{k}}\|^2+(u^kv^ku^{\bar{k}},u^{\bar{k}})+(b,u^{\bar{k}})+a(v^k,u^{\bar{k}})\\
&\le(u^kv^ku^{\bar{k}},u^{\bar{k}})+(b,u^{\bar{k}})+a(v^k,u^{\bar{k}})\\
&\le\|u^kv^ku^{\bar{k}}\|\|u^{\bar{k}}\|+b\|u^{\bar{k}}\|+a\|v^k\|\|u^{\bar{k}}\|\\
&\le(\|u^kv^ku^{\bar{k}}\|+b+a\|v^k\|)\frac{\|u^{k+1}\|+\|u^{k-1}\|}{2},1\le k\le n-1.
\end{aligned}$$

Combining inequality (40), we have

$$\begin{aligned}
&\|u^{k+1}\|-\|u^{k-1}\|\\
&\le 2\tau(\|u^kv^ku^{\bar{k}}\|+b+ac_7),1\le k\le n-1.
\end{aligned}$$

From (36) and (37), we can infer the validity of (35) for $k=0,1$. Assuming that Equation (35) holds when $k=n-1$, namely

$$\|v^{n-1}\|\le c_7,\|u^{n-1}\|\le c_8.$$

Let $k=n-1$, and we have

$$\begin{aligned}
&\|u^n\|-\|u^{n-2}\|\\
&\le c_8^2\tau(\|u^n\|+\|u^{n-2}\|)+2\tau(b+ac_7).
\end{aligned} \tag{41}$$

Taking $\tau\le\frac{1}{c_8^2}-\frac{1}{2}$, (41) becomes

$$\|u^n\|\le(1+4\tau)\|u^{n-2}\|+\frac{4\tau}{c}(b+ac_7).$$

By the Gronwall inequality, it can be derived that

$$\|u^n\| \leq e^{2T}(\|u^0\| + \frac{b+ac_7}{4}) \leq c_{10}e^{2T},$$

and thus, the inequality holds when $k=n$.

By the induction method, we can obtain that (35) holds. □

4.2. The Existence and Uniqueness of Solutions for Our Algorithm

Theorem 2. *The finite difference algorithm (26)–(34) is uniquely solvable.*

Proof. From Equations (32)–(34), u^0, u^1, v^0 and v^1 are uniquely determined. Assuming u^{k-1}, u^k, v^{k-1} and v^k are determined, then the system (26)–(31) yields a system of linear equations for u^{k+1} and v^{k+1}. Consider the homogeneous system of (26)–(31) as follows:

$$\begin{cases} \frac{1}{2\tau}u_0^{k+1} = d_1\frac{1}{h}\delta_x u_{\frac{1}{2}}^{k+1} - \frac{1}{2}u_0^{k+1} + \frac{1}{2}u_0^k v_0^k u_0^{k+1}, & (42) \\ \frac{1}{2\tau}v_0^{k+1} = d_2\frac{1}{h}\delta_x v_{\frac{1}{2}}^{k+1} - \frac{1}{2}(u_0^k)^2 v_0^{k+1} - \frac{1}{2}av_0^{k+1}, & (43) \\ \frac{1}{2\tau}u_i^{k+1} = \frac{1}{2}d_1\delta_x^2 u_i^{k+1} - \frac{1}{2}u_i^{k+1} + \frac{1}{2}u_i^k v_i^k u_i^{k+1}, \quad 1 \leq i \leq m-1, & (44) \\ \frac{1}{2\tau}v_i^{k+1} = \frac{1}{2}d_2\delta_x^2 v_i^{k+1} - \frac{1}{2}(u_i^k)^2 v_i^{k+1} - \frac{1}{2}av_i^{k+1}, \quad 1 \leq i \leq m-1, & (45) \\ \frac{1}{2\tau}u_m^{k+1} = -d_1\frac{1}{h}\delta_x u_{m-\frac{1}{2}}^{k+1} - \frac{1}{2}u_m^{k+1} + \frac{1}{2}u_m^k v_m^k u_m^{k+1}, & (46) \\ \frac{1}{2\tau}v_m^{k+1} = -d_2\frac{1}{h}\delta_x v_{m-\frac{1}{2}}^{k+1} - \frac{1}{2}(u_m^k)^2 v_m^{k+1} - \frac{1}{2}av_m^{k+1}. & (47) \end{cases}$$

Multiplying Equations (42), (44), and (46) by $\frac{1}{2}hu_0^{k+1}$, hu_i^{k+1} and $\frac{1}{2}hu_m^{k+1}$ respectively, and then summing them up, we obtain

$$\begin{aligned} &\frac{1}{2\tau}\|u^{k+1}\|^2 \\ &= -\frac{1}{2}d_1|u^{k+1}|_1^2 - \frac{1}{2}\|u^{k+1}\|^2 + \frac{1}{2}h(\frac{1}{2}u_0^k v_0^k|u_0^{k+1}|^2 + \sum_{i=1}^{m-1} u_i^k v_i^k|u_i^{k+1}|^2 + \frac{1}{2}u_m^k v_m^k|u_m^{k+1}|^2) \\ &\leq \frac{1}{2}h(\frac{1}{2}u_0^k v_0^k|u_0^{k+1}|^2 + \sum_{i=1}^{m-1} u_i^k v_i^k|u_i^{k+1}|^2 + \frac{1}{2}u_m^k v_m^k|u_m^{k+1}|^2). \end{aligned} \tag{48}$$

When u and v have opposite signs, (48) becomes

$$\frac{1}{2\tau}\|u^{k+1}\|^2 \leq 0.$$

Then,

$$\|u^{k+1}\|^2 = 0,$$

that is

$$u^{k+1} = 0.$$

When u and v have the same sign, in conjunction with Theorem 1, Equation (48) becomes

$$\frac{1}{2\tau}\|u^{k+1}\|^2 \leq \frac{c_{11}}{2}\|u^{k+1}\|^2.$$

If $\tau < \frac{1}{c_{11}}$,

$$\|u^{k+1}\|^2 = 0,$$

then,

$$u^{k+1} = 0.$$

Applying similar techniques to v, we obtain

$$v^{k+1} = 0.$$

To sum up, the finite difference algorithm (26)–(31) is uniquely solvable with respect to u^{k+1} and v^{k+1}. $\square$

5. Numerical Results and Discussion

In this section, we use two numerical examples to verify the accuracy and efficiency of our proposed algorithm. All our tests were carried out using MATLAB 2017b running on a Lenovo desktop with 12 GB of RAM and 3.60 GHz CPU.

5.1. Example 1

In this example, let $\{U_i^k, V_i^k | 0 \le i \le m, 0 \le k \le n\}$ be the exact solutions to the Sel$'$kov–Schnakenberg system (2)–(5), and $\{u_i^k, v_i^k | 0 \le i \le m, 0 \le k \le n\}$ be the numerical solutions of the finite difference algorithm (26)–(34), then,

$$\mathcal{U}_i^k = U_i^k - u_i^k, \mathcal{V}_i^k = V_i^k - v_i^k,\ 0 \le i \le m,\ 0 \le k \le n.$$

We denote errors Err and $Err1$ as follows:

$$Err = \sqrt{\|\mathcal{U}\|^2 + \|\mathcal{V}\|^2},$$

and

$$Err1 = \sqrt{\|\mathcal{U}\|^2 + \|\mathcal{V}\|^2 + |\mathcal{U}|_1^2 + |\mathcal{V}|_1^2}.$$

Consider the following Sel$'$kov–Schnakenberg system:

$$\begin{cases} u_t = d_1 \Delta u - u + u^2 v + b + av + f, & (49) \\ v_t = d_2 \Delta v + \lambda - u^2 v - av + g. & (50) \end{cases}$$

where f and g are source term functions of x and t.

We choose the domain $\Omega = (0, 1)$ and take $a = b = 0.01, d_1 = d_2 = 10, \lambda = 5$. Select the solutions as

$$\begin{cases} u(x,t) = (x^2 - x)t^2, \\ v(x,t) = (x^2 - x)t^3. \end{cases}$$

The source term functions f and g can be obtained by bringing the above information into Equations (49) and (50).

We take $M = 1/h$ from 4 to 1024, $\Delta t = 10^{-3}$ with $T = 1$; the numerical results are shown in Table 1. Then, we choose $T = 1$, $N_t = 1/\tau$, varying from 4 to 512 with $h = 1/10{,}000$; the numerical results are shown in Table 2. From Tables 1 and 2, it is evident that our proposed algorithm exhibits second-order accuracy both in space and time.

Table 1. Errors and convergence rates in space for the proposed algorithm.

M	Err	Order	Err1	Order
4	5.1655×10^{-1}	-	5.2581×10^{-1}	-
8	1.2189×10^{-1}	2.08	1.2447×10^{-1}	2.08
16	2.9515×10^{-2}	2.05	3.0190×10^{-2}	2.04
32	7.2559×10^{-3}	2.02	7.4280×10^{-3}	2.02
64	1.7985×10^{-3}	2.01	1.8418×10^{-3}	2.01
128	4.4769×10^{-4}	2.01	4.5853×10^{-4}	2.01
256	1.1171×10^{-4}	2.00	1.1437×10^{-4}	2.00
512	2.7931×10^{-5}	2.00	2.8547×10^{-5}	2.00
1024	7.0136×10^{-6}	1.99	7.1261×10^{-6}	2.00

Table 2. Errors and convergence rates in time for the proposed algorithm.

N_t	Err	Order	Err1	Order
4	5.7535×10^{-3}	-	3.0047×10^{-2}	-
8	1.3799×10^{-3}	2.06	7.2819×10^{-3}	2.04
16	3.3867×10^{-4}	2.03	1.7980×10^{-3}	2.02
32	8.3680×10^{-5}	2.02	4.4489×10^{-4}	2.01
64	2.0720×10^{-5}	2.01	1.0985×10^{-4}	2.02
128	5.1796×10^{-6}	2.00	2.7270×10^{-5}	2.01
256	1.3224×10^{-6}	1.97	6.7907×10^{-6}	2.01
512	3.6489×10^{-7}	1.86	1.6929×10^{-6}	2.00

5.2. Example 2

In this example, we will choose two sets of parameters corresponding to two cases to investigate the spatial patterns of solutions for the system (2)–(5).

For convenience, we can define the average concentration $\bar{u}^n$ and $\bar{v}^n$

$$\begin{cases} \bar{u}^n = \dfrac{1}{m}\displaystyle\sum_{i}^{m} u_i^n, \\ \bar{v}^n = \dfrac{1}{m}\displaystyle\sum_{i}^{m} v_i^n. \end{cases}$$

(Case 1)

Taking the parameters as follows:

$$\lambda = 1, b = 1, a \ = 1, d_1 = 0.1, d_2 = 0.2,$$

it is easy to verify that this aligns with Lemma 2 (1).

Selecting two difference initial value conditions

$$\begin{cases} u^0(x) = 1 + \sin(x), \\ v^0(x) = 1 + \cos(x). \end{cases} \tag{51}$$

$$\begin{cases} u^0(x) = 2, x = 25, \\ u^0(x) = 0, x \neq 25, \\ v^0(x) = 2, x = 75, \\ v^0(x) = 0, x \neq 75. \end{cases} \tag{52}$$

We choose the spatial domain $\Omega = [0, 100]$, the time step $\tau = 0.005$, and the spatial step size $h = 0.5$. Considering two different initial values, we can obtain the snapshots of the concentration at $Nt = 0$, 100, 10,000 and 50,000, respectively, as shown in Figure 1a–h. From Figure 1d,h, we can clearly see that our proposed algorithm is stable and the concentration value of each point is the same.

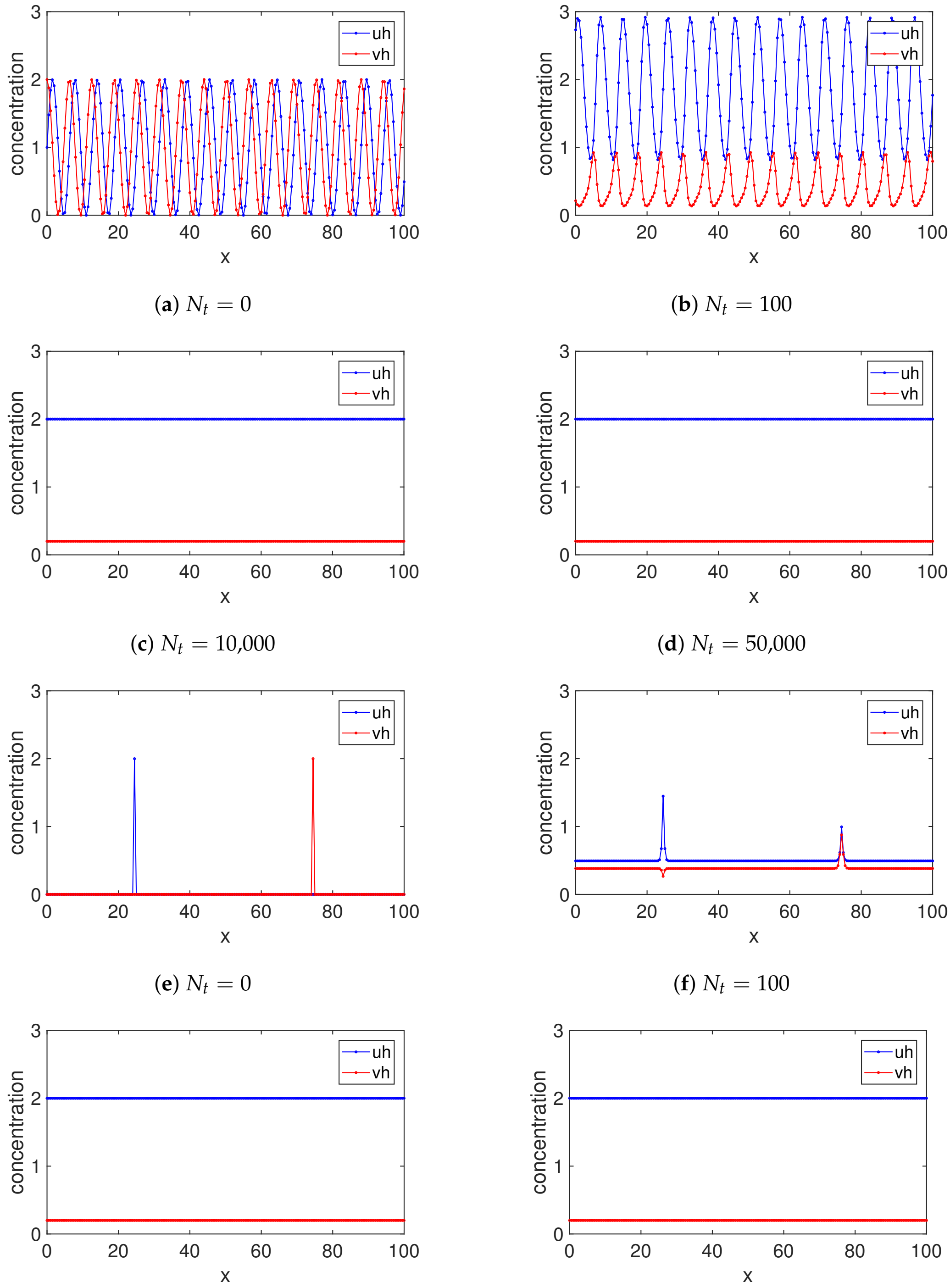

(**a**) $N_t = 0$ (**b**) $N_t = 100$

(**c**) $N_t = 10{,}000$ (**d**) $N_t = 50{,}000$

(**e**) $N_t = 0$ (**f**) $N_t = 100$

(**g**) $N_t = 10{,}000$ (**h**) $N_t = 50{,}000$

Figure 1. Concentration snapshots at different times, (**a**–**d**) under the conditions (51), (**e**–**h**) under the conditions (52), respectively, in case 1.

To investigate the equilibrium points, we calculate the average concentrations $\bar{u}$, $\bar{v}$, u^*, and v^*. We present the concentration evolution diagrams, the average concentration (Figure 2a,c) and the concentration at point $x = 50$ (Figure 2b,d), under two initial value conditions. From Figure 2a,c, we can see that the average concentration quickly reaches the equilibrium point (u^*, v^*). At point $x = 50$, the concentration changes drastically after the beginning.

Finally, for a clearer presentation of the concentration variations, we provide numerical solutions in Figure 3a–d at all time steps under two different initial conditions.

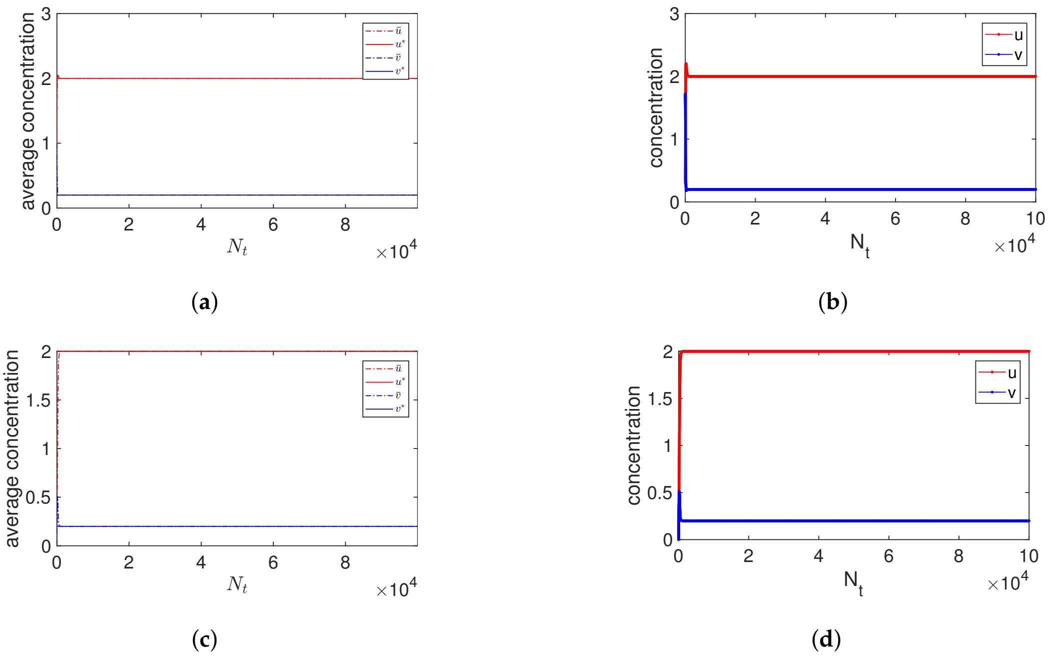

Figure 2. Concentration evolution: (**a**) average concentration, (**b**) concentration at x = 50 under condition (51); (**c**) average concentration, (**d**) concentration at x = 50 under condition (52), in case 1.

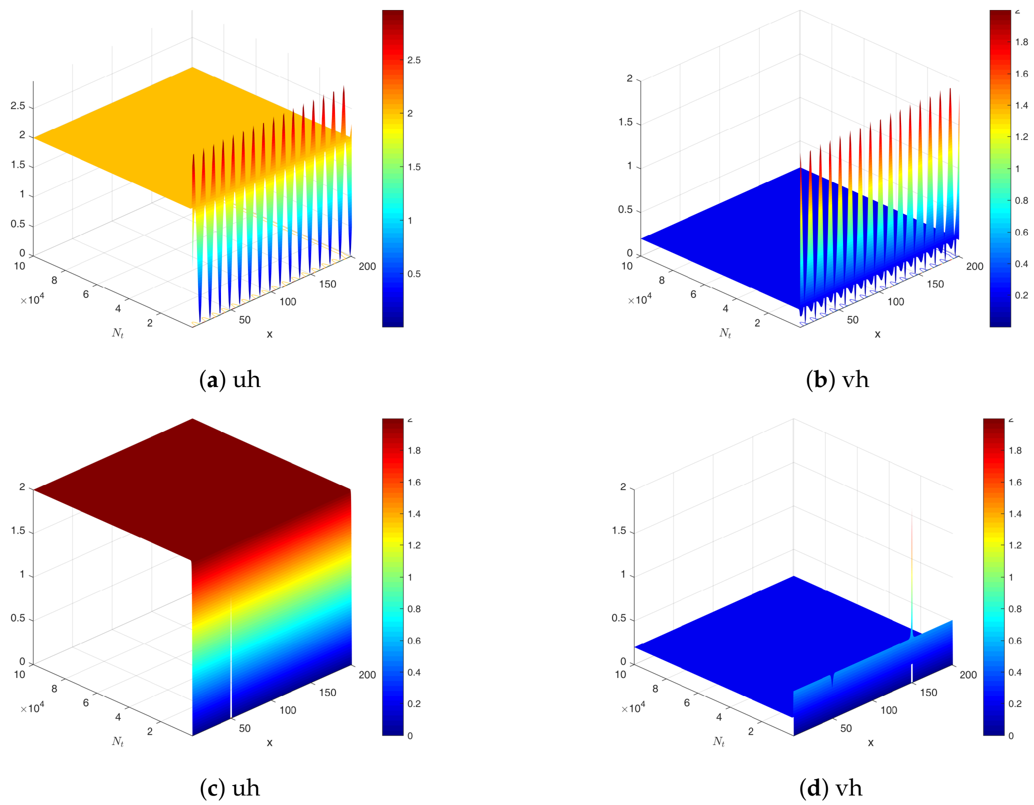

Figure 3. Numerical solutions: (**a**,**b**) under the conditions (51); (**c**,**d**) under the conditions (52), in case 1.

(Case 2)
We consider the following parameters:

$$\lambda = 1.3, b = 0.01, a = 0.01, d_1 = 1.5, d_2 = 25.$$

It can be verified that this conforms to the conditions stated in Lemma 2 (2a).

We choose the spatial domain $\Omega = [0, 100]$ and the time step $\tau = 0.005$, and the space step is chosen as $h = 0.5$. Considering two different initial values, we can obtain the snapshots of the concentration at $Nt = 0, 100, 10,000$ and $100,000$, respectively, as shown in Figure 4a–h. From Figure 4d–h, we can clearly see that our proposed algorithm is stable. Under the initial conditions (51), the solutions tend to reach an equilibrium state more rapidly. The solutions exhibit periodicity in the spatial domain.

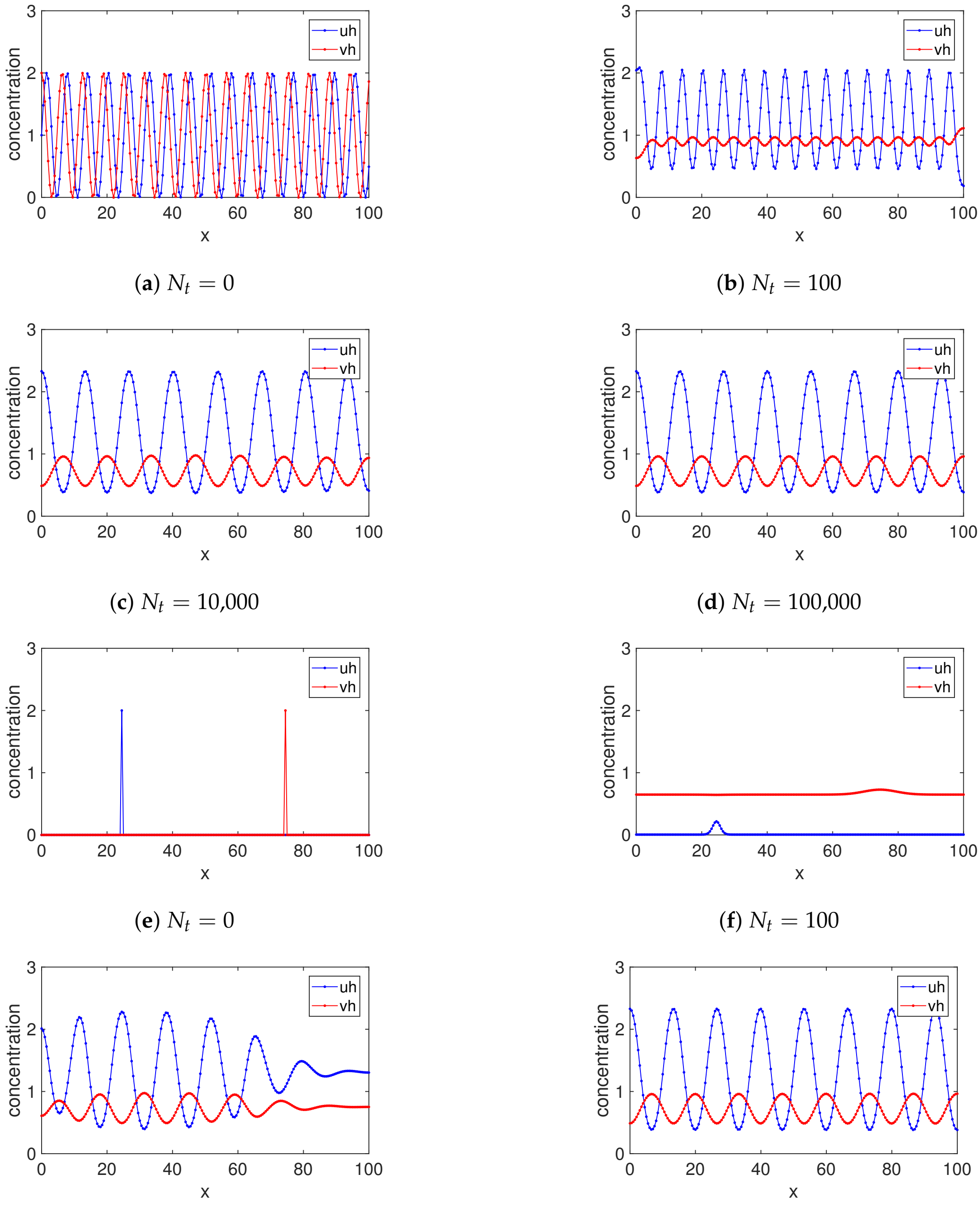

(**a**) $N_t = 0$ (**b**) $N_t = 100$

(**c**) $N_t = 10{,}000$ (**d**) $N_t = 100{,}000$

(**e**) $N_t = 0$ (**f**) $N_t = 100$

(**g**) $N_t = 10{,}000$ (**h**) $N_t = 100{,}000$

Figure 4. Concentration snapshots at different times, (**a**–**d**) under the conditions (51) , (**e**–**h**) under the conditions (52), respectively, in case 2.

Similar to case 1, we calculate the average concentrations $\bar{u}$, $\bar{v}$, u^*, and v^*. We present concentration evolution diagrams, the average concentration (Figure 5a,c) and the concentration at point $x = 50$ (Figure 5b,d), under two initial value conditions. From Figure 5a,c, it is evident that the solution eventually reaches the equilibrium point (u^*, v^*). From Figure 5b,d, it can be observed that the time taken for the solutions to reach the equilibrium point is relatively longer compared to case 1.

Finally, for a clearer presentation of concentration variations, we provide numerical solutions in Figure 6a–d at all time steps under two different initial conditions.

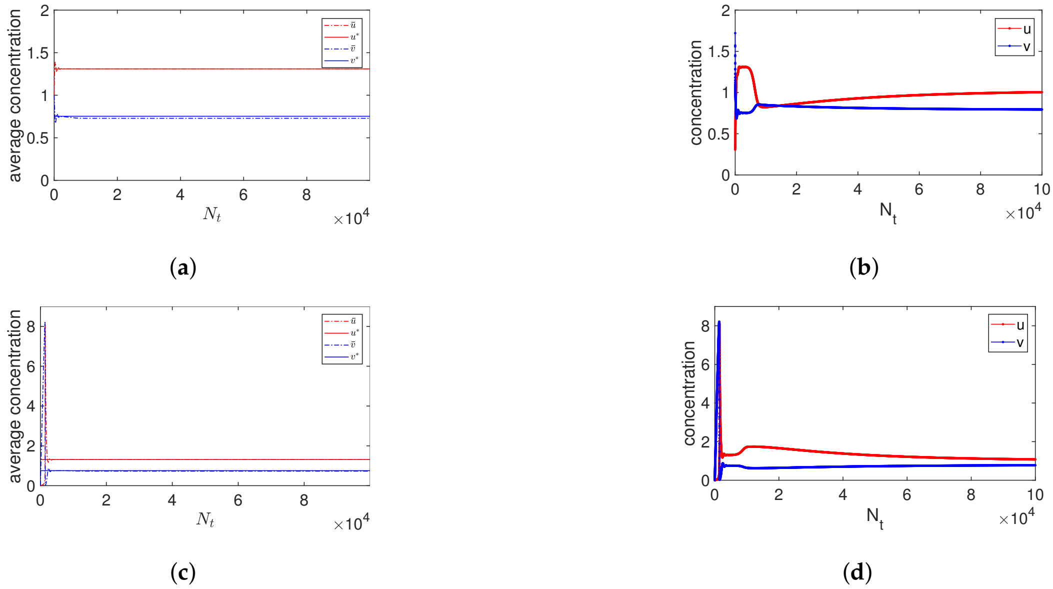

Figure 5. Concentration evolution: (**a**) average concentration, (**b**) concentration at x = 50 under condition (51); (**c**) average concentration, (**d**) concentration at x = 50 under condition (52), in case 2.

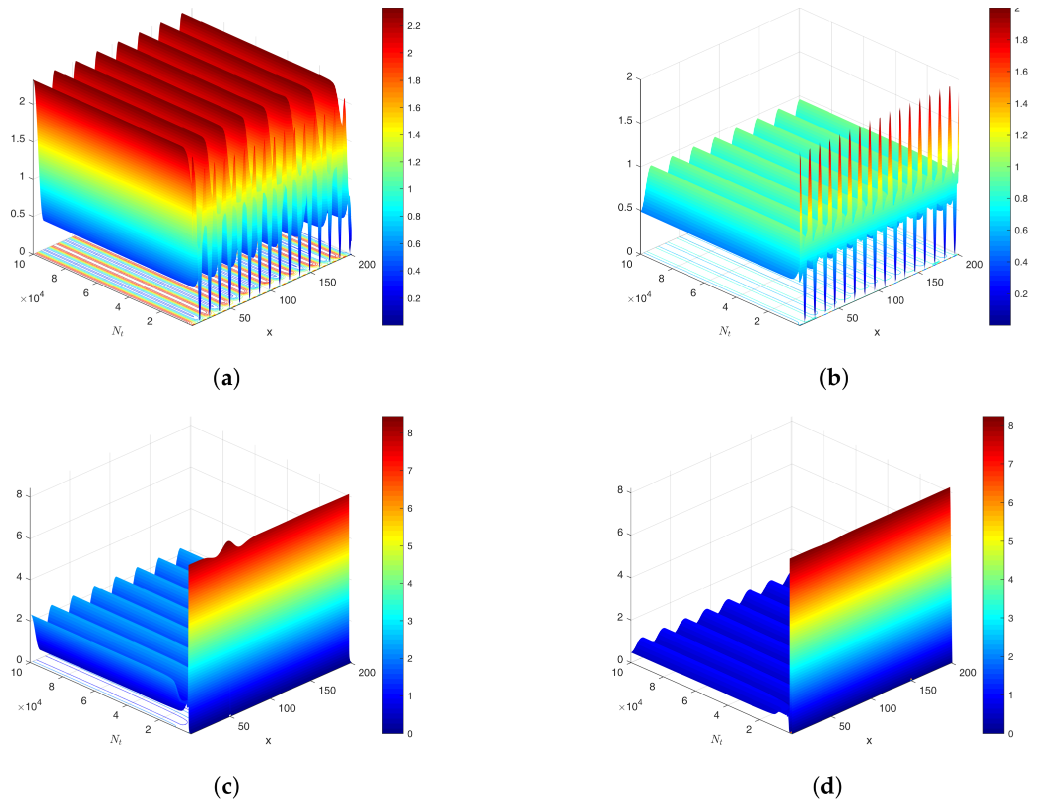

Figure 6. Numerical solutions: (**a**,**b**) under the conditions (51); (**c**,**d**) under the conditions (52), in case 2.

6. Conclusions

An efficient linearized difference algorithm is developed to solve a diffusive Sel$'$kov–Schnakenberg system. We provide a detailed construction process of the algorithm. Proofs for the boundedness of the algorithm solutions, the existence of the algorithm solution and its uniqueness are all provided. Numerical examples validate the efficiency of the algorithm and are consistent with the theoretical analysis results. In the future, we will extend the algorithm to complex nonlinear problems in two and three dimensions and investigate the stability and convergence of the algorithm.

Author Contributions: Y.W.: Conceptualization, Methodology, Validation, Formal analysis, Software, Writing—Original Draft Preparation; X.B.: Conceptualization, Investigation, Supervision. All authors have read and agreed to the published version of the manuscript.

Funding: This research received no external funding.

Data Availability Statement: Data are contained within the article.

Acknowledgments: The authors would like to thank the anonymous referees for many constructive comments and suggestions which led to an improved presentation of this article.

Conflicts of Interest: The authors declare no conflicts of interest.

References

1. Uecker, H.; Wetzel, D. Numerical Results for Snaking of Patterns over Patterns in Some 2D Selkov–Schnakenberg Reaction-Diffusion Systems. *SIAM J. Appl. Dyn. Syst.* **2014**, *13*, 94–128. [CrossRef]
2. Al Noufaey, K. Stability analysis for Selkov-Schnakenberg reaction-diffusion system. *Open Math.* **2021**, *19*, 46–62. [CrossRef]
3. Turing, A.M. The chemical basis of morphogenesis. *Bull. Math. Biol.* **1990**, *52*, 153–197. [CrossRef] [PubMed]
4. Zhao, Y.H.; Iqbal, M.S.; Baber, M.Z.; Inc, M.; Ahmed, M.O.; Khurshid, H. On traveling wave solutions of an autocatalytic reaction–diffusion Selkov–Schnakenberg system. *Results Phys.* **2023**, *44*, 106129. [CrossRef]
5. Goldbeter, A. *Biochemical Oscillations and Cellular Rhythms: The Molecular Bases of Periodic and Chaotic Behaviour*; Cambridge University Press: Cambridge, UK, 1997.
6. Iqbal, M.S.; Seadawy, A.R.; Baber, M.Z. Demonstration of unique problems from Soliton solutions to nonlinear Selkov–Schnakenberg system. *Chaos Solitons Fractals* **2022**, *162*, 112485. [CrossRef]
7. Wang, Y.; Zhou, X.; Jiang, W.; Qi, L. Turing instability and pattern formation in a diffusive Sel'kov–Schnakenberg system. *J. Math. Chem.* **2023**, *61*, 1036–1062. [CrossRef]
8. Sel'Kov, E. Self-Oscillations in Glycolysis 1. A Simple Kinetic Model. *Eur. J. Biochem.* **1968**, *4*, 79–86. [CrossRef] [PubMed]
9. Schnakenberg, J. Simple chemical reaction systems with limit cycle behaviour. *J. Theor. Biol.* **1979**, *81*, 389–400. [CrossRef] [PubMed]
10. Li, B.; Wang, F.; Zhang, X. Analysis on a generalized Sel'kov–Schnakenberg reaction–diffusion system. *Nonlinear Anal. Real World Appl.* **2018**, *44*, 537–558. [CrossRef]
11. Li, Y.; Zhou, Y. Turing–Hopf bifurcation in a general Selkov–Schnakenberg reaction–diffusion system. *Chaos Solitons Fractals* **2023**, *171*, 113473. [CrossRef]
12. Li, B.; Zhang, X. Steady states of a sel'kov-schnakenberg reactin-diffusion system. *Discret. Contin. Dyn. Syst.-Ser. S* **2017**, *10*.
13. Hepson, O.E.; Dag, I. Finite Element Method for Schnakenberg Model. In *Mathematical Methods in Engineering: Applications in Dynamics of Complex Systems*; Springer: Berlin/Heidelberg, Germany, 2019; pp. 41–51.
14. Zhou, J.; Shi, J. Pattern formation in a general glycolysis reaction–diffusion system. *IMA J. Appl. Math.* **2015**, *80*, 1703–1738. [CrossRef]
15. Uecker, H.; Wetzel, D.; Rademacher, J.D. pde2path-A Matlab package for continuation and bifurcation in 2D elliptic systems. *Numer. Math. Theory, Methods Appl.* **2014**, *7*, 58–106. [CrossRef]
16. Sun, Z.Z.; Zhang, Q.; Gao, G.h. *Finite Difference Methods for Nonlinear Evolution Equations*; Walter de Gruyter GmbH & Co KG: Berlin, Germany, 2023; Volume 8.

Disclaimer/Publisher's Note: The statements, opinions and data contained in all publications are solely those of the individual author(s) and contributor(s) and not of MDPI and/or the editor(s). MDPI and/or the editor(s) disclaim responsibility for any injury to people or property resulting from any ideas, methods, instructions or products referred to in the content.